

*Article*

## Thin Layer Drying Kinetics and Mathematical Modeling of Moisture Diffusivity in Cocoa Pod Husk (CPH)

Nattawut Sianoun<sup>a</sup>, Prukraya Pongyeela<sup>b</sup>, Nirana Chairerk<sup>c</sup>, and Juntima Chungsiriporn<sup>d,\*</sup>

Department of Chemical Engineering, Faculty of Engineering, Prince of Songkla University, Songkla, 90110, Thailand

E-mail: <sup>a</sup>s.nattawut64@email.com, <sup>b</sup>prukraya.a@hotmail.com, <sup>c</sup>nirana\_1234@hotmail.com,

<sup>d,\*</sup>juntima.c@psu.ac.th (Corresponding author)

**Abstract.** Cocoa pod husk (CPH), an agricultural by-product of the cocoa separation process, contains an average moisture content of  $5.40 \pm 0.05$  kg<sub>water</sub>/kg<sub>dry matter</sub>. Drying characteristics of CPH were examined in hot air at 50, 60 and 70°C using a laboratory oven with air ventilation at 3 L/min and a load cell sensor (HX-711) was used for weight loss tracking. Twelve mathematical models simulated the drying rate from a drying curve at each operating temperature by comparing four statistically calculated parameters. Levels of variation were investigated by plotting experimental data against the predicted moisture ratios to identify the sum of residuals and obtain a good fit. The Midilli et al. model provided the best drying characteristics with optimized statistical parameters. Using an Arrhenius type relationship, the effective diffusivity coefficient of moisture transfer varied from  $7.979 \times 10^{-10}$  to  $13.298 \times 10^{-10}$  m<sup>2</sup>/s, with operating temperature set at 50, 60 and 70°C and activation energy for moisture diffusion 70.48 kJ/mol.

**Keywords:** Cocoa Pod Husk (CPH), drying characteristics, post-harvest agricultural waste management, effective diffusivities, activation energy, thin layer mathematical model.

**ENGINEERING JOURNAL** Volume 27 Issue 8

Received 15 February 2023

Accepted 7 August 2023

Published 31 August 2023

Online at <https://engj.org/>

DOI:10.4186/ej.2023.27.8.1

## Nomenclature

$a, b, c, g, h, n$	Empirical constant
$k, k_1, k_2$	Drying rate constant (1/min)
$D_e$	Effective diffusivity ( $m^2/s$ )
$D_0$	Pre-exponential factor ( $m^2/s$ )
DR	Drying rate ( $g_{water}/g_{dry\ matter\ min}$ )
$E_a$	Activation energy (kJ/mol)
$M_e$	Equilibrium moisture content ( $g_{water}/g_{dry\ matter\ min}$ )
$M_0$	Initial moisture content ( $g_{water}/g_{dry\ matter\ min}$ )
$M_t$	Moisture content at time $t$ ( $g_{water}/g_{dry\ matter\ min}$ )
MR	Moisture ratio (dimensionless)
$MR_{exp}$	Experimental moisture ratio (dimensionless)
$MR_{pre}$	Predicted moisture ratio (dimensionless)
SSE	Sum of square error
$N$	Number of observations
$n$	Positive integer
$p$	Number of constants
$R$	Universal gas constant (kJ/kmol K)
RMSE	Root mean square error
$R^2$	Coefficient of determination
$T$	Temperature ( $^{\circ}C$ )
$t$	Drying time (min)
$W_0$	Initial weight of dried product (g)
$W_d$	Weight of dried product (g)
$W_t$	Weight of product to be dried at any time (g)
$\chi^2$	Chi-square
EC	Specific energy consumption

## 1. Introduction

Harvesting agricultural products generates copious amounts of waste biomass that require disposal in an eco-friendly and economical manner. The cocoa pod is bulbous and grows along the main and lateral branches of the plant. Cocoa pod husk (CPH), a by-product of cocoa production after removal of the beans, represents 70-80% dry weight of the mature fruit [1] and is produced in large quantities. Each ton of cocoa beans generates ten tons of wet CPH as organic waste dumped at the base of the cocoa plant to decompose into organic fertilizer [2]. Excess volume of CPH causes an oversupply of fertilizer and conversion into other products reduces the cost of waste management and also adds value to agricultural waste. CPH is considered an important energy source that could be used as raw material to produce animal feed instead of maize, soybean meal, rice bran, grits and fish meal [3]. Low-cost animal feed production will provide a competitive advantage because 80% of the cost involves agricultural raw materials. Proximate and chemical analysis revealed that CPH contained 8.6% crude protein, 1.5% lipid, 6.7% ash and 36.6% total dietary fiber, with acid detergent fiber, neutral detergent fiber and total digestible nutrients 43.8%, 56.6% and 60.0%, respectively [4, 5]. Using CPH as the raw material for animal feed production has recently received increased attention, with low cost compared to other agricultural wastes. CPH is a suitable raw material for animal feed production but the high moisture content from AOAC analysis at 84.3% (wet basis) can activate fast decomposition. Drying is the oldest and most widely used method for extending the shelf-life of materials and takes place in two stages [6]. The first phase is moisture evaporation from the material surface into hot air at a steady drying rate. Moisture from the inner material layers diffuses to the outer layers by the driving force of moisture evaporation in the second stage which decreases with time. Important factors affecting the drying process include temperature, relative humidity, rate of ventilation and initial moisture content [7]. Thin layer drying equations classify the drying characteristics of agricultural products into three types as theoretical, semi-theoretical and empirical [8]. The theoretical approach is concerned with either the diffusion equation or the simultaneous heat and mass transfer equation [9], whereas the semi-theoretical and empirical approaches consider only external resistance to mass transfer between materials and ambient air, which is widely used for avoiding the assumption of geometric, mass diffusion and conductivity of materials [10]. Twelve semi-theoretical and empirical models based on the thin layer assumption were used here to study the mechanism of moisture evaporation from CPH. The semi-theoretical models fitted the drying experimental data of the agricultural materials and were based on Newton's law of cooling applied to mass transfer. Assumptions of isothermal and moisture transfer are restricted only at the surface of materials. To study the drying behavior of

materials, the samples must be weighed during the drying process. This involves removing the samples from the drying machine, causing reduced moisture evaporation. The temperature gap between the materials and hot air is high and requires time to heat the sample replaced in the drying machine to regain the set point. To avoid these disturbances, a load cell sensor (HX-711) was used to track material weight reduction using Arduino IDE monitoring that can be manipulated at any range of time intervals to eliminate errors. A lab-scale oven was designed and used to study the drying behavior of CPH. A load cell sensor HX-711 module measuring instrument was installed on the top of the oven to track the moisture reduction rate during the drying process. The load cell sensor avoided disruptions during the drying process from weighing and also provided a high number of measured data points.

The drying processes of other agricultural materials have previously been investigated such as lemon basil leaf [11], thyme leaves [12], scent leaf [11], bitter leaf [13] and elephant apple [14] using fitted mathematical models. These studies used parameters to evaluate the appropriateness of selected models defined by determination coefficients and chi-square. Moisture diffusivity during the drying process and the activation energy required to evaporate the moisture are described by Fick's first law and the Arrhenius type relationship equation, respectively. Gradually increasing the operating temperature positively impacted moisture reduction.

Here, the drying characteristics of CPH were studied as a function of operating temperatures 50, 60 and 70°C, with a constant rate of air ventilation at 3L/min. Under the assumption of thin layer drying materials, the experimental data were fitted with the chosen mathematical models. The effective diffusivity coefficients of moisture transfer and moisture diffusion from the activation energy applied from an Arrhenius type relationship equation were also determined. Statistical parameters including coefficient of determination ( $R^2$ ), reduced chi-square ( $\chi^2$ ), root mean square error (RMSE) and the sum of square errors (SSE) were calculated to ensure model suitability for the CPH drying process.

## 2. Methodology

All material on all pages should fit within an area of A4 (21 x 29.7 cm), 2.8 cm from the top of the page and ending with 2.4 cm from the bottom. The left and right margins should both be 2.4 cm.

### 2.1. Plant Materials

The cocoa fruits of Chumphon hybrid 1 (Pa<sub>7</sub>+Na<sub>32</sub>) were purchased from Tah-Sala in Nakhon Si Thammarat

Province, Southern Thailand. The fruits were washed with tap water to eliminate contaminants and the seeds were separated from the pods by manual cut. Cocoa pod husk (CPH) was cut into small pieces (15 x 15 mm<sup>2</sup>) and 10 mm thickness, kept in a vacuum bag and stored in a freezer at 4°C until use.

### 2.2. Sample Preparation

The CPH was defrosted at ambient temperature to allow equilibration before the experiment. Initial moisture content was determined according to the AOAC (2000) standard by placing 20-30 g of CPH in an aluminum container in a convection dryer at 105°C for 5-6 h. The sample was weighed with a 4 decimal digital weighing scale (Analytical Balance ME204T/00) at time intervals of 30 min. The drying process continued until the sample weight changed by only  $\pm 0.0005$  g. The experiments were triplicated to obtain average moisture content and minimize error.

### 2.3. Drying Oven with HX-711 Load Cell Sensor

An oven chamber with a volume of 0.1215 m<sup>3</sup> (Fig. 1.) was used to study CPH drying behavior. A single perforated tray, 0.045 m<sup>2</sup> surface area, was hung with the load cell sensor (SN-LC-2KG). A strain gauge load cell with a 24-bit analog to digital converter (HX-711) and a 400ms response time was installed on the top of the oven to track sample weight loss on the perforated tray during the drying process. The load cell capacity was 0-2000 g with an accuracy of  $\pm 0.05\%$ . A 300-watt infrared heater was installed as a heat generator inside the oven. The temperature inside the chamber was controlled by a control box that consisted of a type-K thermocouple and a digital screen. Airflow inside the oven was mobilized by an air compressor with a flow rate of 3 L/min. A 6-watt electrical fan was installed on the top of the lab oven to improve air circulation inside the oven. Fresh air from the air compressor was pumped into the bottom of the oven and immediately heated by the heater.

Hot air flowed from the bottom to the top and was drawn out of the lab oven by the electric fan. Samples utilized in each experimental condition weighed  $200 \pm 2$  g. The temperature in each drying process was set in the range 50-70°C with 1°C of temperature increment. For a steady-state system, the oven was warmed for about half an hour before the experiment started. The reduced weight of the sample was real-time tracked by the load cell sensor and monitored by Arduino IDE. The load cell sensor was recalibrated before starting each experiment to avoid numerical errors.

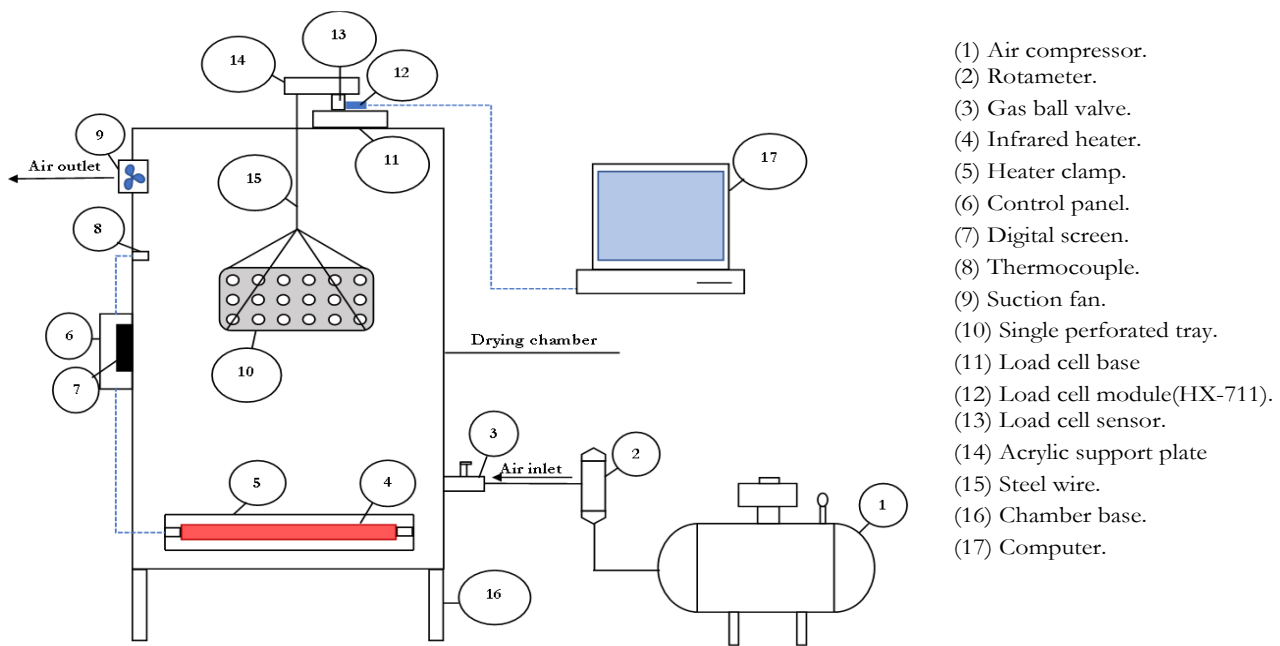


Fig. 1. Experimental set-up.

## 2.4. Experimental Procedure

Drying experiments were performed at 50, 60 and 70°C in the convective dryer attached to the load cell sensor. The perforated tray was weighed with a digital balance and used as a reference for load cell sensor calibration. Two hundred grams of square pieces of CPH with a thickness of 10 mm and an initial moisture content of 540.03% (dry basis, DB) were uniformly separated in the perforated tray while hanging with the load cell sensor. The time interval was tracked by the load cell sensor and monitored by Arduino IDE at 15 min intervals to observe the reduction in CPH weight. The CPH drying process in each set was carried out until moisture content was reduced to 169% (dry basis, DB). The experiment was performed in triplicate for each run.

## 2.5. Drying Mathematical Models

Empirical equations have been previously used to support and describe the drying kinetics of an agricultural product. Most of the models were considered based on the assumption of thin layer drying. Reduction in moisture content during the drying process was used as raw data to express the drying rate as a function of time. The integral drying rate was expressed in terms of critical time and optimal drying process time was obtained. Empirical models were used to explain the heat perforation in materials under hot air drying, with reduction in moisture content tracked by a load cell sensor connected to the HX-711 module with response time of 600 ms. Raw data were monitored by Arduino IDE to explain the drying kinetics of thin layer CPH through empirical equations. The following assumptions were made.

- I. Negligible heat and mass losses: Significant heat losses to the surroundings and mass losses, except for moisture removal, are negligible.
- II. Uniform drying conditions: Drying conditions (temperature, humidity, airflow) are assumed to be uniform throughout the system.
- III. Single component drying: The material being dried is primarily composed of a single component, typically water, which is the focus of moisture removal.

Moisture content can be written in terms of moisture ratio (MR) on a dry basis (DB) to easily observe the drying process. The moisture ratio (MR) at any time  $t$  can be obtained from Eq. (1):

$$MR = MR_e + (MR_i - MR_e)f(t, a, b), \quad (1)$$

where a term of  $(t, a, b)$  is a function of time, and fitting parameters ( $a$  and  $b$ ). To simplify the equation, Eq. (1) can be expressed as the dimensionless moisture ratio at any time  $t$  as follows:

$$MR = f(t, a, b) \quad (2)$$

$$MR = \frac{M_t - M_e}{M_i - M_e} \quad (3)$$

Considering that the equilibrium moisture content ( $M_e$ ) is considerably smaller in magnitude compared to  $M_t$  and  $M_i$ , the equilibrium moisture content can be neglected, as suggested by Thakor et al. (1999). Thus, the term of moisture ratio can be written as:

$$MR = \frac{M_t}{M_i} \quad (4)$$

where MR is the final moisture ratio,  $M_t$ , and  $M_i$  are any time (t), and initial moisture content respectively. Empirical equations that serve the assumptions and satisfy the result are given in Table 1.

## 2.6. Correlation Coefficients and Error Analyses

Many statistical parameters have been used to evaluate the appropriate model for describing the drying mechanism including the correlation coefficient ( $R^2$ ). This parameter is the primary criterion used as a tool to support the appropriate selection, while reduced chi-square ( $\chi^2$ ) and root mean square error (RMSE) values are also considered. The goodness of fit mathematical model of the result gives higher  $R^2$  but lower  $\chi^2$  and RMSE are preferred. As shown in Eq. (5), the reduced chi-square ( $\chi^2$ ) obtained from calculating the mean square deviations between the calculated value and the experiment value was also considered. The reduced chi-square ( $\chi^2$ ) can be calculated as follows:

$$\chi^2 = \frac{\sum_{i=1}^N (MR_{exp,i} - MR_{pre,i})^2}{(N-n)} \quad (5)$$

The root mean square error (RMSE) is shown in Eq. (6):

$$RMSE = \sqrt{\frac{1}{N} \sum_{i=1}^N (MR_{exp,i} - MR_{pre,i})^2} \quad (6)$$

where  $MR_{exp,i}$  is the moisture content obtained from the number of experiments,  $MR_{pre,i}$  is the calculated result as predicted moisture content,  $N$  is the number of data points and  $n$  is the number of constants used to fit the selected model.

$$MR = \frac{8}{\pi^2} \sum_{n=0}^{\infty} \frac{1}{(2n+1)^2} \exp\left(-\frac{(2n+1)^2 \pi^2 D_{eff} t}{4L_0^2}\right) \quad (7)$$

where  $D_{eff}$  is the effective diffusivity ( $m^2/s$ ) and  $L_0$  is the half thickness of slab object (m). For an extended drying period, the first term of Eq. (7) can be simplified to the logarithmic term, as shown in Eq. (8):

$$\ln MR = \ln \frac{8}{\pi^2} - \frac{\pi^2 D_{eff} t}{4L_0^2} \quad (8)$$

The determination of diffusivity can be obtained by plotting experimental data from the drying process in terms of the natural logarithm of MR as a function of unit time (t) in Eq. (8). A slope obtained from this plot is shown in Eq. (9) as follows:

$$\text{Slope} = \frac{\pi^2 D_{eff}}{4L_0^2} \quad (9)$$

Table. 1. Selected mathematical models for thin layer drying of CPH.

Model no	Model name	Model equation	Reference
1	Lewis	$MR = \exp(-kt)$	[15]
2	Page	$MR = \exp(-kt^n)$	[16]
3	Modified Page-I	$MR = \exp[(-kt)^n]$	[17]
4	Henderson and Pabis	$MR = a \cdot \exp(-kt)$	[18]
5	Wang and Singh	$MR = 1 + at + bt^2$	[19]
6	Logarithmic	$MR = a \cdot \exp(-kt) + c$	[20]
7	Two term	$MR = a \cdot \exp(-k_1 t) + b \cdot \exp(-k_2 t)$	[21]
8	Two term exponential	$MR = a \cdot \exp(-kt) + (1-a) \cdot \exp(-kat)$	[22]
9	Modified Henderson and Pabis	$MR = a \cdot \exp(-kt) + b \cdot \exp(-gt) + c \cdot \exp(-ht)$	[23]
10	Midilli et al.	$MR = a \cdot \exp(-kt^n) + bt$	[24]
11	Approximation of diffusion	$MR = a \cdot \exp(-kt) + (1-a) \cdot \exp(-kbt)$	[25]
12	Verma et al.	$MR = a \cdot \exp(-kt) + (1-a) \cdot \exp(-gt)$	[26]

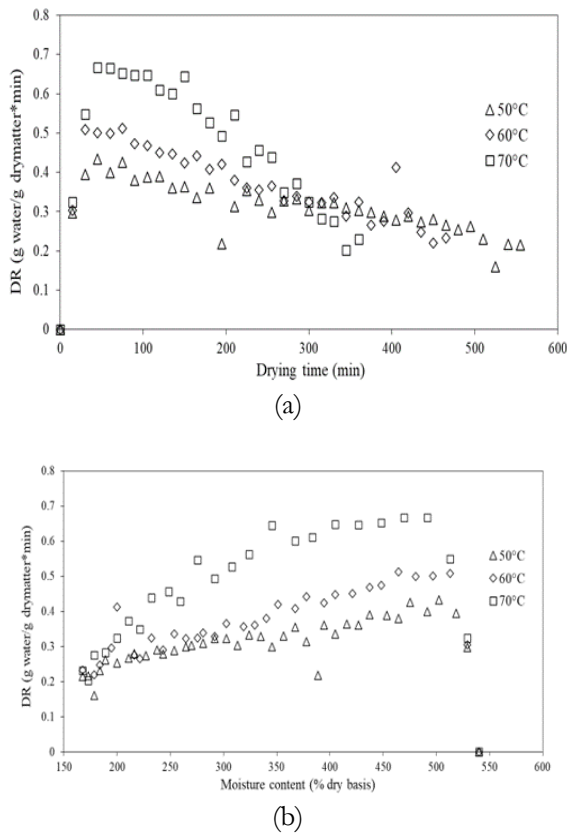


Fig. 2. Variation of drying rate with (a) drying time and (b) moisture content of CPH.

## 2.7. Calculation of Activation Energy

The Arrhenius-type equation is applicable in describing the temperature dependency of drying rate or moisture content reduction. Although originally developed for chemical reactions, it can be adapted for drying kinetics. The effective diffusivity is also dependent on the temperature, and can be described by an Arrhenius-type relationship equation as follows:

$$D_{\text{eff}} = D_0 \exp\left(-\frac{E_a}{RT}\right) \quad (10)$$

where  $D_0$  is the pre-exponential factor of the Arrhenius equation ( $\text{m}^2/\text{s}$ ),  $E_a$  is the activation energy ( $\text{kJ}/\text{mol}$ ),  $R$  is the universal gas constant ( $\text{kJ}/\text{mol K}$ ) and  $T$  is the absolute temperature ( $\text{K}$ ). Equation (10) can be simplified by plotting  $\ln D_{\text{eff}}$  versus the reciprocal of the absolute temperature ( $1/T$ ). The linearity of Eq. (10) is shown in Eq. (11). The slope obtained from the plot represents the activation energy in the Arrhenius equation.

$$\ln D_{\text{eff}} = \ln D_0 - \frac{E_a}{RT} \quad (11)$$

## 2.8. Specific Energy Consumption

The specific energy consumption (SEC) equation is represented below.

$$\text{SEC} = \frac{\text{Total electrical power supplied in drying}}{\text{Amount of water removed during drying}}, \frac{\text{kWh}}{\text{kg}} \quad (12)$$

where  $P_{\text{total}}$  is a total electric power that is supplied in the drying process, this term can be expressed as equation below.

$$P_{\text{total}} = P_{\text{heater}} + P_{\text{fan}} + P_{\text{sensor}} + P_{\text{control box}} + P_{\text{compressor}}, \quad (13)$$

[kWx 3,600s]

where  $P_{\text{heater}}$  is the electric power supplied to the heater,  $P_{\text{fan}}$  is the electric supplied to the fan for air ventilation,  $P_{\text{sensor}}$  is the electric supplied to the sensor which used to track the reduction of moisture content during the drying process,  $P_{\text{control box}}$  is the electric power supplied to the control gadgets which used to adjust the heater to set point,  $P_{\text{compressor}}$  is the electric supplied to the compressor to generate air flow through the system.

## 3. Main Text Results and Discussions

### 3.1. Drying Curves

CPH contained an initial moisture content of  $5.40 \pm 0.05$  kg of water per kg of dry matter and thickness of 10 mm as a thin layer. CPH was dried at 50, 60 and 70°C in a convective dryer attached to a load cell sensor. The CPH equilibrium moisture content was  $1.67 \pm 0.01$  kg of water per kg of dry matter, while the weight did not change. Reduction in moisture content of CPH during the drying process at each temperature is shown in Fig. 3. Moisture content decreased continually as drying time increased. Drying times that reached equilibrium moisture content for CPH samples were 555, 465 and 360 min at 50, 60 and 70°C, respectively. This result concurred with Wang et al. (2007) who studied drying temperature range of 75-105°C and Tunde-Akintunde et al. (2011) who studied drying temperature range of 40-80°C. A constant rate period of the drying process did not appear but falling rate period occurred throughout the drying process. This phenomenon was induced by the mechanism of liquid and/or vapor diffusion and caused moisture movement in the CPH samples [27]. As expected, the constant rate of air ventilation did not affect drying time but increase in operating temperature led to reduction in drying time. Accelerating the rate of moisture evacuation from the surface by increasing heat transfer between CPH materials and dried air caused increase in moisture diffusion from the inner layer to the surface of materials. Experimental results revealed that operating temperature was the most important factor that influenced drying time. The drying rate (DR) can be expressed as the amount of evaporated moisture over time ( $\text{g}_{\text{water}}/\text{g}_{\text{dry matter}} \cdot \text{min}$ ). Figure 2(a) shows the variation of drying rate versus drying time and Fig. 2(b) shows moisture content (% dry basis) of the CPH samples at 50, 60 and 70°C at 3 L/min, respectively. After the initial period of the drying process, the drying rate reached its

maximum value. Afterward, the CPH samples dried during the falling rate period. Initial values of drying rate increased when the operating temperature increased. An increase in temperature from 50°C to 70°C caused the maximum drying rate of 77% from 0.42 to 0.64  $\frac{\text{g}_{\text{water}}}{\text{g}_{\text{dry matter}} \cdot \text{min}}$ . Moisture evaporation initially occurred on the surface of the CPH samples, but this phenomenon became less important as drying time increased. Moisture diffusion from the inner layers of CPH samples progressively increased. Our experimental results concurred with other studies related to the drying process of agricultural and vegetable products: [28] for quince, [29] for banana, [30] for pumpkin, [31] for apricot, [32] and [24] for mushroom, pistachio, and pollen.

### 3.2. Fitting the Mathematical Models

Curve fitting in MATLAB software was used to plot the experimental moisture ratio (MR) data from the drying process in each condition as a function of time. Twelve semi-theoretical models that have been widely used in literature to explain the kinetics of the drying process were selected, as shown in Table 1. Non-linear regression techniques were used to attain the values of constants in each model. The goodness of fit was evaluated by calculating parameters including the coefficient of determination ( $R^2$ ), the reduced chi-square ( $\chi^2$ ), root mean square error (RMSE) and the sum of square errors (SSE). The calculated statistical parameters

are shown in Table 2. The results demonstrated that the Midilli model provided the best statistical values, with an  $R^2$  of over 0.999 for all operating temperatures, while magnitudes of  $\chi^2$  and RMSE were lowest compared with the other models; between  $1.226 \times 10^{-5}$  and  $1.892 \times 10^{-5}$  for  $\chi^2$  and between 0.00344 and 0.00430 for RMSE. The SSE of this model presented values between 0.00140 and 0.0034, indicating that the Midilli model offered the best approximation for the experimental data.

Figure 3 shows different selected model fits with moisture ratio versus drying time at each temperature 50, 60 and 70°C of the drying process. The prediction of moisture ratio during the drying process calculated from the selected models was both under and over the experimental data curve. Figure 4(a) compares the experimental and predicted moisture ratio values at different temperatures by the Midilli model. Results showed that the trending line concurred with the experimental data, with all magnitudes ranging around the 45° line as very good acceptance between predicted and experimental data [27]. This result indicated that the Midilli model effectively forecast the mechanism of moisture evaporation of the CPH samples during the drying process and provided the highest value of desired values, as well as the lowest value of undesired statistical values. The Midilli model also provided the lowest value of the sum of residuals as most suitable for the CPH drying process.

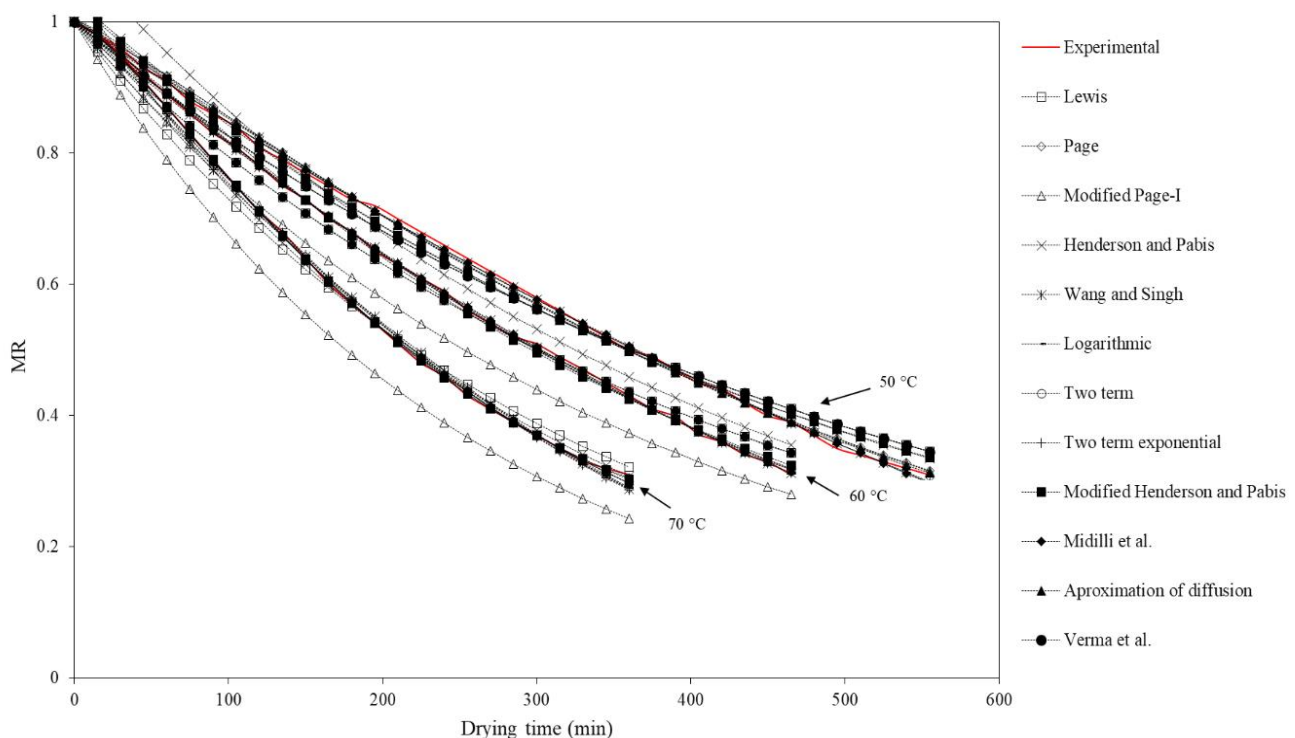


Fig. 3. Variation of experimental and forecasted moisture ratio with drying time for different operating air temperatures.

Table 2. Curve fitting boundary of the semi-theoretical thin layer models for CPH (3 L/min at 50, 60 and 70°C of operating temperature).

Model no	Model constants	R <sup>2</sup>	$\chi^2$	RMSE	SSE
50°C					
1	k = 0.001918	0.9889	4.668 x 10 <sup>-4</sup>	0.0216	0.0859
2	k = 0.0007266, n = 1.166	0.9983	7.021 x 10 <sup>-5</sup>	0.0083	0.0128
3	k = 0.002038, n = 1.166	0.9983	7.021 x 10 <sup>-5</sup>	0.0083	0.0128
4	a = 1.036, k = 0.002035	0.9937	2.683 x 10 <sup>-4</sup>	0.0163	0.0488
5	a = -0.001587, b = 5.849 x 10 <sup>-7</sup>	0.9995	2.000 x 10 <sup>-5</sup>	0.0045	0.0036
6	a = 1.701, c = -0.6975, k = 0.0009644	0.9996	1.917 x 10 <sup>-5</sup>	0.0043	0.0035
7	a = 0.04432, b = 0.9544, k <sub>1</sub> = 0.001867, k <sub>2</sub> = 0.001917	0.9989	4.594 x 10 <sup>-5</sup>	0.0067	0.0082
8	a = 0.9987, k = 0.001918	0.9889	4.720 x 10 <sup>-4</sup>	0.0216	0.0859
9	a = 0.9981, b = 0.0325, c = 1.136 x 10 <sup>-6</sup> , g = 0.002015, h = 4.535, k = 0.002019	0.9934	2.848 x 10 <sup>-4</sup>	0.0166	0.0496
10	a = 1.008, b = -0.0003868, k = 0.001528, n = 0.9645	0.9996	1.892 x 10 <sup>-5</sup>	0.0043	0.0034
11	a = -4.095, b = 0.878, k = 0.003718	0.9989	4.727 x 10 <sup>-5</sup>	0.0068	0.0085
12	a = 0.03899, g = 0.001918, k = 0.001917	0.9888	4.772 x 10 <sup>-4</sup>	0.0217	0.0859
60°C					
1	k = 0.002303	0.9929	3.038 x 10 <sup>-4</sup>	0.0174	0.0480
2	k = 0.001078, n = 1.134	0.9994	2.663 x 10 <sup>-5</sup>	0.0051	0.0042
3	k = 0.002415, n = 1.134	0.9994	2.663 x 10 <sup>-5</sup>	0.0051	0.0042
4	a = 1.034, k = 0.002434	0.9971	1.248 x 10 <sup>-4</sup>	0.0111	0.0195
5	a = -0.00197, b = 1.056 x 10 <sup>-6</sup>	0.9994	2.594 x 10 <sup>-5</sup>	0.0051	0.0041
6	a = 1.328, c = -0.3151, k = 0.001612	0.9997	1.465 x 10 <sup>-5</sup>	0.0038	0.0023
7	a = 2.713, b = -1.707, k <sub>1</sub> = 0.003481, k <sub>2</sub> = 0.00441	0.9995	2.226 x 10 <sup>-5</sup>	0.0047	0.0034
8	a = 0.0001208, k = 19.05	0.9929	3.090 x 10 <sup>-4</sup>	0.0175	0.0482
9	a = 0.01478, b = 1.073, c = -0.08557, g = 0.002574, h = 0.03127, k = 0.03148	0.9978	9.585 x 10 <sup>-5</sup>	0.0096	0.0142
10	a = 1.011, b = -0.0001964, k = 0.00174, n = 1.02	0.9997	1.456 x 10 <sup>-5</sup>	0.0038	0.0022
11	a = -1.36, b = 0.7404, k = 0.004676	0.9994	2.518 x 10 <sup>-5</sup>	0.0050	0.0039
12	a = 0.0005609, g = 0.002303, k = 0.002305	0.9928	3.117 x 10 <sup>-4</sup>	0.0175	0.0480
70°C					
1	k = 0.00316	0.9898	5.218 x 10 <sup>-4</sup>	0.0228	0.0699
2	k = 0.001385, n = 1.151	0.9979	1.076 x 10 <sup>-4</sup>	0.0104	0.0143
3	k = 0.0738, n = 0.04282	0.9898	5.258 x 10 <sup>-4</sup>	0.0229	0.0699
4	a = 1.051, k = 0.003403	0.9972	1.441 x 10 <sup>-4</sup>	0.0120	0.0192
5	a = -0.002755, b = 2.266 x 10 <sup>-6</sup>	0.9959	2.097 x 10 <sup>-4</sup>	0.0145	0.0279
6	a = 1.118, c = -0.07633, k = 0.003007	0.9976	1.224 x 10 <sup>-4</sup>	0.0111	0.0162
7	a = 0.0536, b = 0.9937, k <sub>1</sub> = 0.003398, k <sub>2</sub> = 0.00339	0.9971	1.483 x 10 <sup>-4</sup>	0.0122	0.0194
8	a = 0.000316, k = 9.996	0.9897	5.306 x 10 <sup>-4</sup>	0.0230	0.0706
9	a = 1.086, b = 0.5003, c = -0.5839, g = 0.0519, h = 0.04902, k = 0.003553	0.9992	4.268 x 10 <sup>-5</sup>	0.0065	0.0055
10	a = 1.001, b = 0.0002907, k = 0.0008479, n = 1.281	0.9997	1.299 x 10 <sup>-5</sup>	0.0036	0.0017
11	a = -0.08671, b = 0.09683, k = 0.03671	0.9992	4.201 x 10 <sup>-5</sup>	0.0065	0.0055
12	a = 1.087, g = 0.03674, k = 0.003555	0.9992	4.201 x 10 <sup>-5</sup>	0.0065	0.0055

### 3.3. Determination of Effective Diffusivities

The experimental results can be explained by Fick's diffusion equation. Slab geometry is an assumption of materials at each temperature of the drying process. The diffusion coefficient was determined by plotting the result of the experiment in terms of  $\ln(MR)$  as a function of drying time. Figure 4(b) shows a plot of  $\ln(MR)$  as a sloped straight line. The slope values were used to calculate the effective diffusivities according to Eq. (9) as the measurement of the effective diffusivity. Effective diffusivities of dried CPH samples at each operating temperature of 50, 60 and 70°C were  $7.979 \times 10^{-10}$ ,  $9.499 \times 10^{-10}$  and  $13.298 \times 10^{-10} \text{ m}^2/\text{s}$ , respectively. As expected, the increment in the operating temperature generated  $D_e$  values which increased because increase in operating temperature caused reduction in drying time. Values were in the typical range of  $10^{-10}$  to  $10^{-9} \text{ m}^2/\text{s}$  for vegetables and agricultural materials and comparable to results in the literature as  $1.6260 \times 10^{-9}$  to  $4.3612 \times 10^{-9} \text{ m}^2/\text{s}$  for drying apricots between 50 and 80°C [31], drying sludge from olive oil extraction range  $2.224 \times 10^{-10}$  to  $6.993 \times 10^{-10} \text{ m}^2/\text{s}$  between 20 and 80°C [27] and drying apple pomace range  $2.026 \times 10^{-9}$  to  $3.935 \times 10^{-9} \text{ m}^2/\text{s}$  between 75 and 105°C [19].

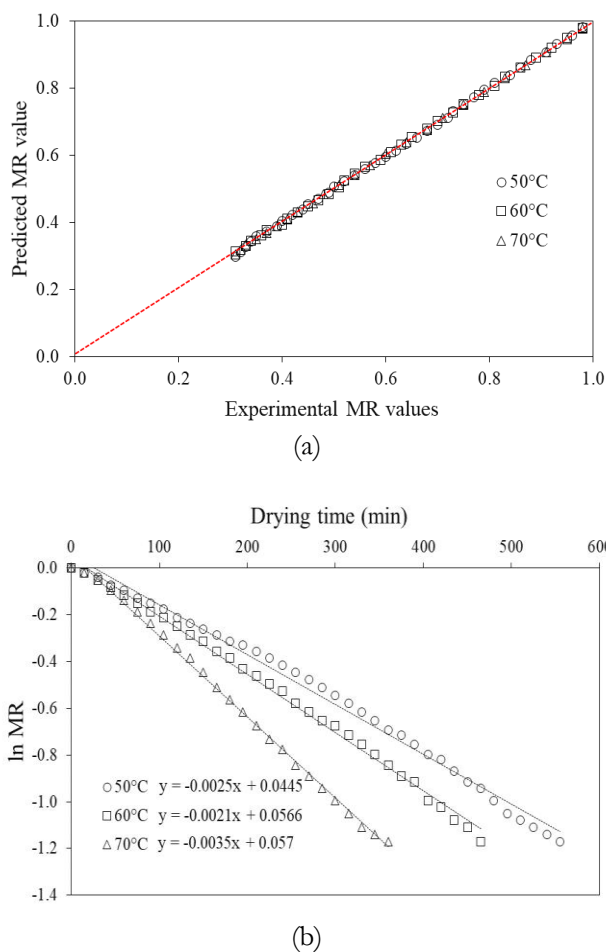


Fig. 4. (a) Plot of predicted MR value with experimental values and (b) plot of  $\ln(MR)$  with drying time.

### 3.4. Activation Energy

Correlations between conditions of the drying process and calculated values of effective diffusivity ( $D_e$ ) were expressed by an Arrhenius type equation according to Eq. (10) using the value of the gas constant  $8.3143 \text{ kJ/kmol K}$ . To obtain the magnitudes of the coefficients,  $\ln D_e$  was plotted against the reciprocal of each operating temperature. The slope represented  $-E_a/R$ , while the intercept was  $\ln(D_0)$ , as shown in Fig. 4(b) The value of activation energy obtained from the calculation was  $70.48 \text{ kJ/kmol}$ , while the value of the Arrhenius pre-exponential factor was  $4.814 \times 10^{-6} \text{ m}^2/\text{s}$ . As predicted, activation energy of the drying process increased as sample thickness on the trays increased. This should be considered when designing drying machines and calculating the amount of energy required to remove moisture from the materials. Compares the activation energy estimated in our study and previous investigations of other materials such as sludge of olive extraction  $15.77 \text{ kJ/mol}$  [27], olive cake  $26.71 \text{ kJ/mol}$  [33], lemon basil leaf  $32.34 \text{ kJ/mol}$  [11], okra  $51.26 \text{ kJ/mol}$  [6], green bun  $39.47 \text{ kJ/mol}$  [34], black tea  $406.02 \text{ kJ/mol}$  [8], thyme leaves  $21.40 \text{ kJ/mol}$  [12], red peppers  $42.80 \text{ kJ/mol}$  [21], and carrot  $28.36 \text{ kJ/mol}$  [35]. Activation energy required for moisture diffusion of CPH was higher than other agricultural materials but lower than the activation energy of black tea. Activation energy consumption is influenced by the physical structure of the samples. For example, CPH has a hard outer layer as a barrier for moisture diffusion and consists of high moisture content. This requires higher energy consumption than other materials.

### 3.5. Electrical Energy Consumption, Drying Time and Analysis of Specific Energy Consumption (SEC)

Figure 5(a) shown the energy consumption from experiments, the energy consumption used for 50,60, and 70°C of drying process was 3.7, 5.0, and 5.4 MJ respectively, so the highest temperature of drying process consumed highest energy while the best result with concern to the energy consumption is founded from the 50°C of drying temperature. Figure 5(b) shows the specific energy consumption in each operation temperature of drying process. The difference of specific energy consumption occurred because of the first state of drying process. The moisture on the CPH surface is evaporated while the interior is still wet; the dry surface as outer layer resists the heat transport, causing in a reduction of drying and evaporation rate, also effecting long period of time to reach expected moisture content. Even though the lowest temperature in this study required the longest drying time compared to the other values, it was still the optimal solution when the energy evaluation was taken into consideration.

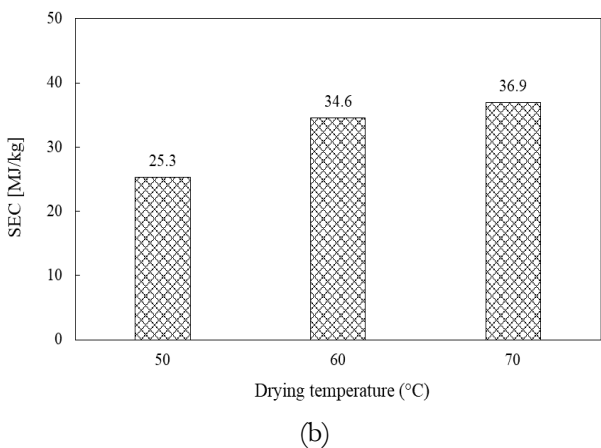
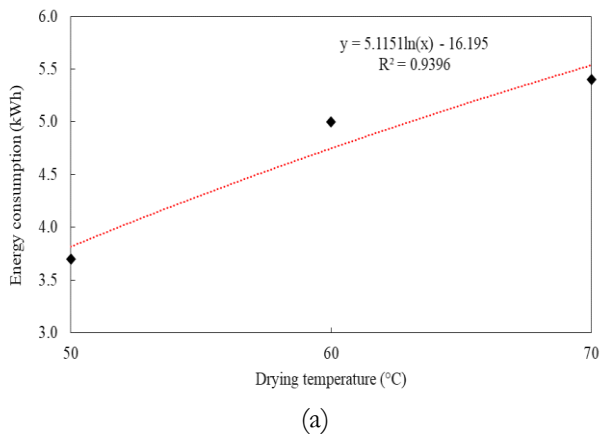


Fig. 5. (a) Energy consumption in each drying temperature (b) Specific energy consumption in each drying temperature.

#### 4. Conclusions

In this study, CPH pieces (15 x 15 x 10 x mm<sup>3</sup>) obtained from the cocoa separation process were successfully investigated using the drying process. The initial moisture content of CPH samples was 5.40 kg<sub>water</sub>/kg<sub>dry matter</sub> ± 0.5%. Twelve mathematical experimental models based on the assumption of thin layer drying kinetics were used to explain the drying behavior of CPH pieces and investigated in the temperature range 50–70°C. Results revealed that the Midilli model exhibited the best drying characteristics of CPH pieces, with high statistical values of R square, RMSE, SSE and reduced chi-square. The rate of air ventilation was set at 3L/min and results showed that the operating temperature had an impact on drying time. Moisture ratio in the CPH pieces was reduced by increasing the drying temperature and time. The drying results were recorded by a load cell using sensor tracking and the reduction rates of moisture in the CPH pieces indicated that the Midilli model gave the best fit for the drying curves. The graphic of the drying curves showed that values of effective diffusivity ranged between 7.979 x 10<sup>-10</sup> and 13.298 x 10<sup>-10</sup> m<sup>2</sup>/s with activation energy of CPH pieces 70.48 kJ/mol. The optimal drying conditions

could be used to design an oven for a future pilot-scale test.

#### Acknowledgement

The authors are thankful for the scholarship support through Songklanakarin Graduate Student Scholarship from the Prince of Songkla University (PSU), Graduate School Research Support Funding, and facilities and equipment support from the Discipline of Excellence in Department of Chemical Engineering, Department of Chemical Engineering, Faculty of Engineering, Prince of Songkla University.

#### References

- [1] K. P. P. Nair, "Cocoa (*Theobroma cacao* L.)," in *The Agronomy and Economy of Important Tree Crops of the Developing World*. Elsevier, 2010, ch. 5, pp. 131-180.
- [2] Z. S. Vásquez, D. P. de Carvalho Neto, G. V. M. Pereira, L. P. S. Vandenberghe, P. Z. de Oliveira, P. B. Tiburcio, H. L. G. Rogez, A. Góes Neto, and C. R. Soccol, "Biotechnological approaches for cocoa waste management: A review," *Waste Management*, vol. 90, pp. 72–83, 2019. [Online]. Available: <https://doi.org/10.1016/j.wasman.2019.04.030>
- [3] E. O. K. Oddoye, C. K. Agyente-Badu, and E. Gyedu-Akoto, "Cocoa and its by-products: Identification and utilization," in *Chocolate in Health and Nutrition*. Humana Press Inc., 2013, pp. 23–37.
- [4] A. Donkoh, C. C. Atuahene, B. N. Wilson, and D. Adomako, "Chemical composition of cocoa pod husk and its effect on growth and food efficiency in broiler chicks," *Anim Feed Sci Technol.*, vol. 35, pp. 161–169, 1991. [Online]. Available: [https://doi.org/10.1016/0377-8401\(91\)90107-4](https://doi.org/10.1016/0377-8401(91)90107-4)
- [5] E. M. Aregheore, "Chemical evaluation and digestibility of cocoa (*Theobroma cacao*) byproducts fed to goats," *Trop Anim Health Prod.*, vol. 34, pp. 339–348, 2002. [Online]. Available: <https://doi.org/10.1023/A:1015638903740>
- [6] I. Doymaz, "Drying characteristics and kinetics of okra," *J. Food Eng.*, vol. 69, pp. 275–279, 2005. [Online]. Available: <https://doi.org/10.1016/j.jfoodeng.2004.08.019>
- [7] J. F. Richardson, J. H. Harker, and J. R. Backhurst, "Drying," in *Chemical Engineering*, 5th ed. Oxford: Butterworth-Heinemann, 2002, ch. 16, pp. 901-969.
- [8] P. C. Panchariya, D. Popovic, A. L. Sharma, "Thin-layer modelling of black tea drying process," *J. Food Eng.*, vol. 52, pp. 349–357, 2002. [Online]. Available: [https://doi.org/10.1016/S0260-8774\(01\)00126-1](https://doi.org/10.1016/S0260-8774(01)00126-1)
- [9] F. T. Ademiluyi and M. F. N. Abowei, "Theoretical model for predicting moisture ratio during drying of spherical particles in a rotary dryer," *Modelling and Simulation in Engineering*, vol. 2013, 2013. [Online]. Available: <https://doi.org/10.1155/2013/491843>

- [10] P. Alvarez and P. Legues, "A semi-theoretical model for the drying of Thompson seedless grapes," *Drying Technology*, vol. 4, pp. 1–17 (1986). [Online]. Available: <https://doi.org/10.1080/07373938608916308>
- [11] N. N. Mbegbu, C. O. Nwajinka, and D. O. Amaefule, "Thin layer drying models and characteristics of scent leaves (*Ocimum gratissimum*) and lemon basil leaves (*Ocimum africanum*)," *Heliyon*, vol. 7, p. e05945, 2021. [Online]. Available: <https://doi.org/10.1016/j.heliyon.2021.e05945>
- [12] O. Y. Turan and F. E. Firatligil, "Modelling and characteristics of thin layer convective air-drying of thyme (*Thymus vulgaris*) leaves," *Czech Journal of Food Sciences*, vol. 37, pp. 128–134, 2019. [Online]. Available: <https://doi.org/10.17221/243/2017-CJFS>
- [13] R. H. Gumus, "Drying characteristics and kinetics of bitter leaf (*Vernonia amygdalina*) and scent leaf (*Ocimum gratissimum*)," *Chemical and Process Engineering Research*, vol. 32, pp. 1–11, 2015.
- [14] S. Nag and K. K. Dash, "Mathematical modeling of thin layer drying kinetics and moisture diffusivity study of elephant apple," *Int Food Res J.*, vol. 23, pp. 2594–2600, 2016.
- [15] D. M. Bruce, "Exposed-layer barley drying: Three models fitted to new data up to 150°C," *Journal of Agricultural Engineering Research*, vol. 32, pp. 337–348, 1985. [Online]. Available: [https://doi.org/10.1016/0021-8634\(85\)90098-8](https://doi.org/10.1016/0021-8634(85)90098-8)
- [16] G. E. Page, "Factors influencing the maximum rates of air drying shelled corn in thin layers," M.S. thesis, Purdue University, 1949.
- [17] G. M. White, I. J. Ross, and C. G. Poneleit, "Fully-exposed drying of popcorn," *Transaction of the American Society of Agricultural Engineers*, vol. 24, no. 2, pp. 466–469, 1981.
- [18] S. M. Henderson, "Progress in developing the thin layer drying equation," *Transactions of the American Society of Agricultural Engineers*, vol. 17, pp. 1–3, 1974. [Online]. Available: <https://doi.org/10.13031/2013.37052>
- [19] Z. Wang, J. Sun, X. Liao, F. Chen, G. Zhao, J. Wu, and X. Hu, "Mathematical modeling on hot air drying of thin layer apple pomace," *Food Research International*, vol. 40, pp. 39–46, 2007. [Online]. Available: <https://doi.org/10.1016/j.foodres.2006.07.017>
- [20] I. T. Togrul and D. Pehlivan, "Mathematical modelling of solar drying of apricots in thin layers," *J. Food Eng.*, vol. 55, pp. 209–216, 2002. [Online]. Available: [https://doi.org/10.1016/S0260-8774\(02\)00065-1](https://doi.org/10.1016/S0260-8774(02)00065-1)
- [21] F. Kaymak-Ertekin, "Drying and rehydrating kinetics of green and red peppers," *J. Food Sci.*, vol. 67, pp. 168–175, 2002. [Online]. Available: <https://doi.org/10.1111/j.1365-2621.2002.tb11378.x>
- [22] Y. I. Sharaf-Eldeen, J. L. Blaisdell, and M. Y. Hamdy, "Model for ear corn drying," *Transactions of the American Society of Agricultural Engineers*, vol. 23, 1980. [Online]. Available: <https://doi.org/10.13031/2013.34757>
- [23] V. T. Karathanos, "Determination of water content of dried fruits by drying kinetics," *J. Food Eng.*, vol. 39, pp. 337–344, 1999. [Online]. Available: [https://doi.org/10.1016/S0260-8774\(98\)00132-0](https://doi.org/10.1016/S0260-8774(98)00132-0)
- [24] A. Midilli, H. Kucuk, and Z. Yapar, "A new model for single-layer drying," *Drying Technology*, vol. 20, pp. 1503–1513, 2002. <https://doi.org/10.1081/DRT-120005864>
- [25] O. Yaldiz, C. Ertekin, and H. I. Uzun, "Mathematical modeling of thin layer solar drying of sultana grapes," *Energy*, vol. 26, pp. 457–465, 2001. [Online]. Available: [https://doi.org/10.1016/S0360-5442\(01\)00018-4](https://doi.org/10.1016/S0360-5442(01)00018-4)
- [26] M. F. Hutjens and J. H. Baltz, "Keeping extension programs current in order to meet the needs of a dynamic dairy industry," *J. Dairy Sci.*, vol. 83, pp. 1412–1417, 2000. [Online]. Available: [https://doi.org/10.3168/jds.S0022-0302\(00\)75010-7](https://doi.org/10.3168/jds.S0022-0302(00)75010-7)
- [27] A. R. Celma, S. Rojas, F. López, I. Montero, and T. Miranda, "Thin-layer drying behaviour of sludge of olive oil extraction," *J. Food Eng.*, vol. 80, pp. 1261–1271, 2007. [Online]. Available: <https://doi.org/10.1016/j.foodeng.2006.09.020>
- [28] M. J. Barroca and R. P. F. Guiné, "Study of drying kinetics of quince," in *Proceedings of International Conference of Agricultural Engineering CIGR-AgEng*, 2012. vol. 2012, pp. 2–7.
- [29] A. O. Omolola, A. I. O. Jideani, and P. F. Kapila, "Drying kinetics of banana (*Musa spp.*)," *Interciencia*, vol. 40, pp. 374–380, 2015.
- [30] T. Y. Tunde-Akintunde and G. O. Ogunlakin, "Mathematical modeling of drying of pretreated and untreated pumpkin," *J. Food Sci. Technol.*, vol. 50, pp. 705–713, 2013. [Online]. Available: <https://doi.org/10.1007/s13197-011-0392-2>
- [31] S. Faal, T. Tavakoli, and B. Ghobadian, "Mathematical modelling of thin layer hot air drying of apricot with combined heat and power dryer," *J. Food Sci. Technol.*, vol. 52, pp. 2950–2957, 2015. [Online]. Available: <https://doi.org/10.1007/s13197-014-1331-9>
- [32] L. Valadez-Carmona, C. P. Plazola-Jacinto, M. Hernández-Ortega, M. D. Hernández-Navarro, F. Villarreal, H. Necochea-Mondragón, A. Ortiz-Moreno, and G. Ceballos-Reyes, "Effects of microwaves, hot air and freeze-drying on the phenolic compounds, antioxidant capacity, enzyme activity and microstructure of cacao pod husks (*Theobroma cacao* L.)," *Innovative Food Science and Emerging Technologies*, vol. 41, pp. 378–386, 2017. [Online]. Available: <https://doi.org/10.1016/j.ifset.2017.04.012>

- [33] I. Doymaz, O. Gorel, and N. A. Akgun, "Drying characteristics of the solid by-product of olive oil extraction," *Biosyst Eng.*, vol. 88, pp. 213–219, 2004. [Online]. Available: <https://doi.org/10.1016/j.biosystemseng.2004.03.003>
- [34] W. Senadeera, B. R. Bhandari, G. Young, and B. Wijesinghe, "Influence of shapes of selected vegetable materials on drying kinetics during fluidized bed drying," *J. Food Eng.*, vol. 58, pp. 277–283, 2003. [Online]. Available: [https://doi.org/10.1016/S0260-8774\(02\)00386-2](https://doi.org/10.1016/S0260-8774(02)00386-2)
- [35] I. Doymaz, "Convective air drying characteristics of thin layer carrots," *J. Food Eng.*, vol. 61, pp. 359–364 2004. [Online]. Available: [https://doi.org/10.1016/S0260-8774\(03\)00142-0](https://doi.org/10.1016/S0260-8774(03)00142-0)



**Nattawut Sianoun** received a B.Eng degree in Chemical engineering (2018) from Prince of Songkla university. He is a Ph.D candidate of Dual Degree Programs in chemical engineering at Prince of Songkla university, and expected to graduate in 2023.



**Prukraya Pongyeela** received a B.Sc degree in Science (Chemistry) in 2008 from Prince of Songkla university, and M.E. of chemical engineering (2011) from Prince of Songkla university. She is working as a researcher at the faculty of engineering in Prince of Songkla university.



**Nirana Chairerk** received a B.Sc degree in Science (Chemical engineering) in 2014 from Walailuk university, and M.E. of chemical engineering (2018) from Prince of Songkla university. She is working as a researcher at the faculty of engineering in Prince of Songkla university.



**Juntima Chungsiriporn** received a B.Eng degree in Chemical engineering (1993) and M.S. degree in Chemical engineering (1999) from Prince of Songkla university, and Ph.D. degree of Energy and Environment from JGSEE. Associate Professor Juntima is working as a lecturer at chemical engineering, Prince of Songkla university.